XVI IMEKO World Congress
Measurement - Supports Science - Improves Technology - Protects Environment ... and Provides Employment - Now and in the Future
Vienna, AUSTRIA, 2000, September 25-28

MULTI-AXIS STRAIN STATE SENSOR BASED ON OPTICAL FIBER TECHNOLOGY

T. Rossmanith, X.D. Jin and J.S. Sirkis
Smart Materials and Structures Research Center
University of Maryland at College Park, College Park, MD 20742, USA

Abstract: This paper describes a single micro-optical fiber sensor capable of measuring four strains simultaneously in a composite structure. This single transducer is based on cascading four micro Fabry-Pérot cavities to measure three normal strains and one shear strain in the plane of the optical fiber cross-section. The development of the sensor fabrication and signal processing techniques are discussed. This fabrication includes designing and fabricating new optical fibers, optical fiber circuits, and an optical fiber multi-strain sensor head. This paper presents 2D and 3D finite element analysis to establish the transformation between fiber core and composite host strain states.

Keywords: optical fiber three-strain sensor, Fabry-Pérot Interferometer, path matched differential interferometry, finite element analysis, micromechanics analysis

1 INTRODUCTION

Embedding optical fiber sensors to provide a measure of the internal strain state is a concept that has recently seen extensive research. However, uniquely relating the change in optical properties to internal strain components, even axial strain, has been much more difficult than first imagined. The difficulties are many fold, but the most important is that all intrinsic fiber optic sensor configurations produce an optical response that is functionally dependent on three orthogonal strain components, rather than a single strain component. Thus far there have been only few successful attempts documented [1-3] in the open literature using a single fiber optic sensor to simultaneously measure more than one strain component. Lo and Sirkis [1] were able to measure two orthogonal strain components by simultaneously making interferometric and polarimetric measurements in a single fiber segment. Jin *et al*. [2] cascaded a Bragg grating with an ILFE sensor to measure two orthogonal strain components. This sensor concept is much less complex than that proposed by Lo and Sirkis [1], and was notable in that the sensor was embedded in a composite cantilever beam. Recently, Udd *et al*. [3] proposed a concept of using two Bragg gratings with different pitches written into stress-induced high-birefringent (HiBi) optical fiber to measure three strain components and temperature. In Udd et al.'s proposed sensor [3], each Bragg grating results in two reflected Bragg wavelengths, one corresponding to each of the polarization axes of the HiBi fiber. This sensor results in four reflected Bragg wavelengths. Their idea is to measure the response of the four peaks in the reflected spectrum and formulate a system of four equations for temperature and three orthogonal strain components. Preliminary data was presented to justify the concept [3], but they have not yet implemented their sensor design.

We propose a single micro-optical fiber sensor capable of simultaneously measuring four key elements of the complete strain state at one point in composite material. The strain components include the normal strain parallel to the optical fiber axis, the secondary principal strains in the plane perpendicular to the optical fiber axis, and the orientation of the secondary principal plane. This paper describes progress in developing the sensor system, sensor fabrication and signal processing techniques, mechanical and optical sensor design, and finite element analysis of the micromechanics.

2 OPTICAL ARRANGEMENT

2.1 Technical Approach

The sensor configuration is shown schematically in Figure 1, and is based on cascading four very short gage length Fabry-Pérot sensors fabricated from different types of optical fibers. The Fabry-Pérot cavities are produced from hollow core, circular core and two sections of side-hole fibers, which are rotated at an angle of 45° relative to each other. These types of fiber are selected because each

has a completely different optical response to strain, therefore enabling four independent optical measurements to be used to solve for the three normal strains and one in-plane shear strain. The first of the Fabry-Pérot cavities is a standard intrinsic Fabry-Pérot (IFP) sensor fabricated from standard circular core fiber. The partially reflecting internal mirror [4] on the left and an air/glass interface on the right form the sensing cavity. The second cavity is fabricated by fusing a hollow core fiber between two segments of standard circular core fiber, where the air/glass interfaces create the reflective surfaces (4%) that form the cavity. This configuration is known as an In-Line Fiber Etalon (ILFE) [5]. The other two Fabry-Pérot sensors are fabricated from specifically fabricated side-hole fibers.

The hollow core Fabry-Pérot (ILFE) sensor is sensitive only to axial strain, so its optical signal directly provides the axial strain. The standard fiber Fabry-Pérot sensor has an isotropic sensitivity to transverse strain, while the side-hole fiber Fabry-Pérot sensors have an anisotropic sensitivity to strain. The two side-hole cavities are oriented at 45° relative to each other so that the stress state in the core of the two cavities would be different in response to the same strain state in the composite host. Using the ILFE sensor to provide direct information about the axial strain has the important advantage of potentially reducing the requisite micromechanics to a two-dimensional analysis. This would considerably reduce the complexity of the micromechanics analysis that is required to determine the strains in the composite structures from sensor readings. As a result, the optical signals from the standard and the side-hole fiber sensors lead to the two transverse strains and one in-plane shear strain.

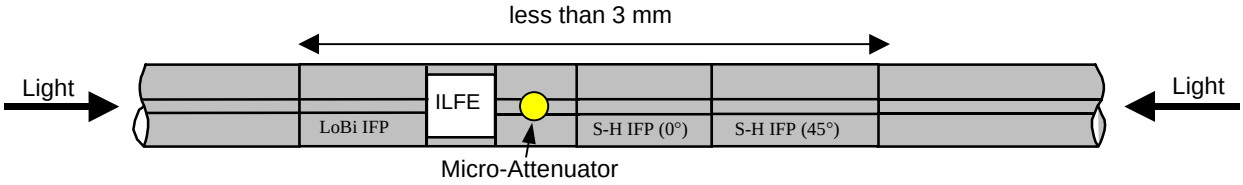

Figure 1. Schematic of proposed multi-strain micro sensor.

The signal from each of the four cascaded Fabry-Pérot sensors are accessed using coherence division multiplexing through the use of four path matched read-out interferometers, as will be discussed in Section 2.3. Note however, that the signal exiting the respective read-out interferometers must still be demodulated in order to extract the four unambiguous phase signals. This aspect of the optical arrangement is also discussed in Section 2.3.

The sensor configuration in Figure 1 shows the ILFE/IFP cavities separated from the two side-hole cavities by a micro-attenuator. Multiplexing cross talk analysis completed with the constraint of maintaining the sensor length less than 3mm lead to the conclusion that selecting the four cavity lengths to reduce the cross-talk to acceptable levels is extremely difficult. As a result, a sensor configuration was designed so that only two serialized Fabry-Pérot cavities must be multiplexed at one time. In this configuration, light is launched into the multi-strain sensor from both directions. The light launched from the left side is intended to interrogate only the ILFE and LoBi IFP components, whereas the light launched from the right side is intended to interrogate the two side-hole IFP sensors. The micro-attenuator prevents the two counter-propagating electro-magnetic fields from interacting with the wrong Fabry-Pérot cavities.

2.2 Side-Hole Fiber Design

A review of the literature suggested that optical side-hole fibers are a suitable choice for an optical fiber with anisotropic response to transverse strains [6,7]. As a result, a 2D finite element analysis was conducted with a PANDA-like side-hole fiber.

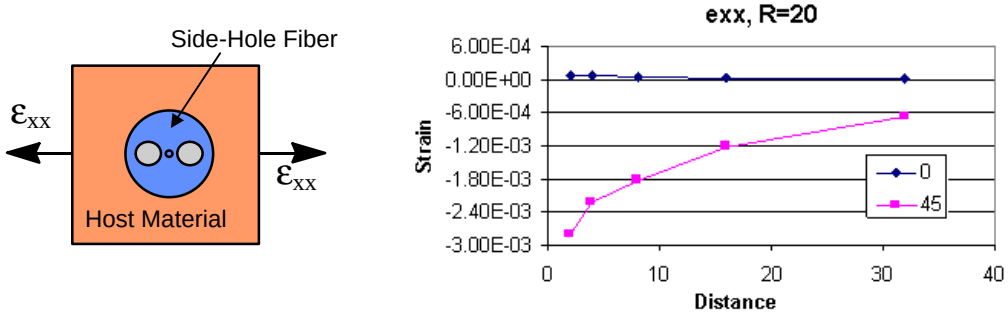

Figure 2. The x-axis strain in the side-hole fiber. The geometry of side-hole fiber is shown on the left, and the graph gives typical results of the FEM.

This parametric study of the PANDA fiber is used to optimize its geometry. While the diameter of the fiber is 125 μm and the diameter of the fiber core is 5.6 μm, the radius of two holes and the distance between the fiber core and each hole are assumed to be design variables. The results are provided in Figure 2 for only ε_{xx} strains and indicate that when the radius of the two holes is larger than 10 μm and the distance is less than 20 μm, the strains in the cores of fibers oriented at 0° and 45° will have a significant difference.

2.3 Multiplexing and Demodulation Techniques

Demodulation is the electro-optic system required to convert the intensity signal recorded by photodetectors to unambiguous phase change signals. The difficulties primarily arise from the frequency response limitations of many of the electro-optic devices used for phase-modulation. Also, virtually all demodulation schemes were developed for high sensitivity phase measurements, and are therefore not capable of accommodating even moderate phase changes. As a result, passive quadrature demodulation techniques will be used.

The optical arrangement uses to interrogate a single micro-cavity sensor is shown in Figure 3. The demodulation scheme used path matched differential interferometry (PMDI) to yield two quadrature shifted intensity signals [8]. Algorithms that allow the extraction of the strain-induced phase change from these two signals take advantage of the inverse tangent function [9]. When the read-out interferometer length is chosen to be within the length of the sensor cavity, the typical interference intensity function is given by

$$I_1 = A_1 + B_1 \cos\left(\frac{4p}{l_0} L_s - f_0\right), \tag{1}$$

where L_s is the cavity length of the sensor; $f_0 = 4pL_{r1}/l_0$, where L_{r1} is the cavity length of the first read-out interferometer, A_1 is a DC term independent from coherent interference, and B_1 is the interference fringe visibility. The second read-out interferometer is used much in the same way as the first, except special care is taken to yield a sine function instead of a cosine function by choosing the cavity length of the second read-out interferometer to be $L_{r2} = L_{r1} + (2m+1)\,l_0/8$, where m is an integer. In this case f_0 becomes $f_0+p/2$. Then the interference intensity functions of the both read-out interferometers can be rewritten as

$$\begin{aligned} I_1 &= A_1 + B_1 \cos\Delta f \\ I_2 &= A_2 + B_2 \sin\Delta f \end{aligned} \tag{2}$$

where $Df = 4pL_s e_{zz}/l_0$ is the strain-induced phase change. Once the cosine and sine functions in above equations have been obtained, the strain can be easily determined by using the following simple arctangent function

$$e_{zz} = \frac{l}{4pL} \tan^{-1}\left(\frac{I_2}{I_1}\right). \tag{3}$$

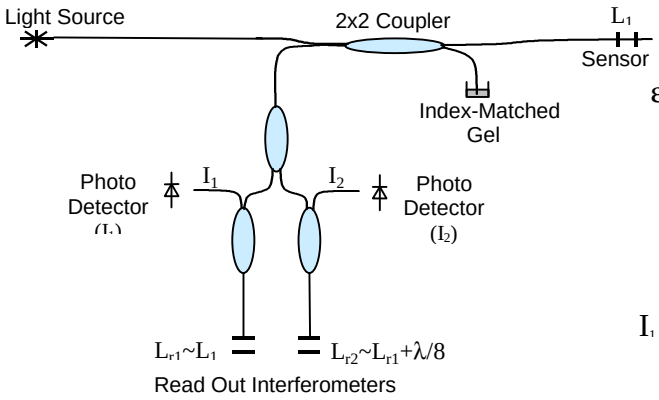

Figure 3. Optical arrangement for a single micro cavity sensor.

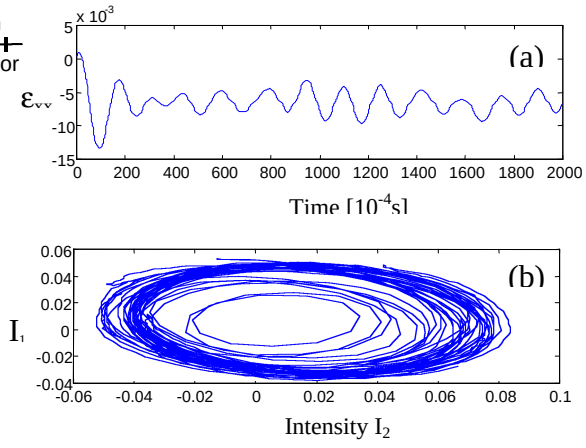

Figure 4. the strain and the corresponding I_1/I_2-graph for a micro Fabry-Pérot cavity.

The strain is determined from the strain-induced phase change using the phase-strain model for the sensor. Figure 4 shows the strain signal of applied impact at a micro Fabry-Pérot cavity and two corresponding quadrature shifted intensity signals I_1 and I_2. Using PMDI-based coherence division multiplexing [8] combined with the passive demodulation requires eight read-out interferometers to simultaneously interrogate the four cavity sensors. To reduce the size and cost of the optical system, all read-out interferometers are being fabricated using MEMS (Micro-Electro Mechanical Systems) technology, which allows us to reduce an entire array of bulk interferometers to fit on a single chip [10, 11].

3 MICROMECHANICS

Micromechanics analysis has been applied to the multi-strain sensor to help design the transducer, and to develop a relationship between the strains in the fiber sensor and the far-field strains in the host material. The sensor consists of one ILFE sensing cavity, one standard fiber IFP cavity and two cascaded IFP cavities with two side-holes each. The principal angles of the two side-hole sensors are oriented at 45° relative to each other. The IFP sensors produced from non-standard fibers present significant mechanics challenges because by choice, they produce complex stress distributions in the core [12]. This, coupled with the fact that the stress distribution may be discontinuous at the interfaces between Fabry-Pérot cavities, suggests that a three dimensional analysis is required. A three-dimensional analysis requires significant computational effort, and therefore two-dimensional approaches that capture the requisite strain state information are very desirable. As noted in Section 2.1, adding the ILFE sensor to the system reduces the solution for the transverse strains to a two-dimensional problem, which again motivates a search for two-dimensional solutions. Several analysis techniques were investigated. These include two-dimensional and three-dimensional finite element analysis, and two dimensional closed-form semi-analytical techniques.

3.1 Comparison of 3D and 2D finite element results

Three-dimensional finite element analysis can provide accurate and reliable strain distribution predictions for the multi-axis sensor embedded in a composite structure. On the other hand, the geometry of optical fiber sensor, its small cross-section compared with sensor length, and the fact that the ILFE sensor gives direct information about the external strain suggests that 2D models might provide desired results with a much smaller computational penalty. To verify this assumption, a comparison between 3D and 2D finite element analysis of the multi-strain sensor was performed. The host material is assumed to be a unidirectional composite with fiber direction along the optical fiber direction. Silica optical fiber and the polyamide coating around it are isotropic materials.

Figure 5 shows the 3D results of strain distributions in the cross-sectional plane (*x*-*y* plane) of the sensor core as a function of position along optical fiber axis for a composite subjected to a uniform tension in *x*-direction.

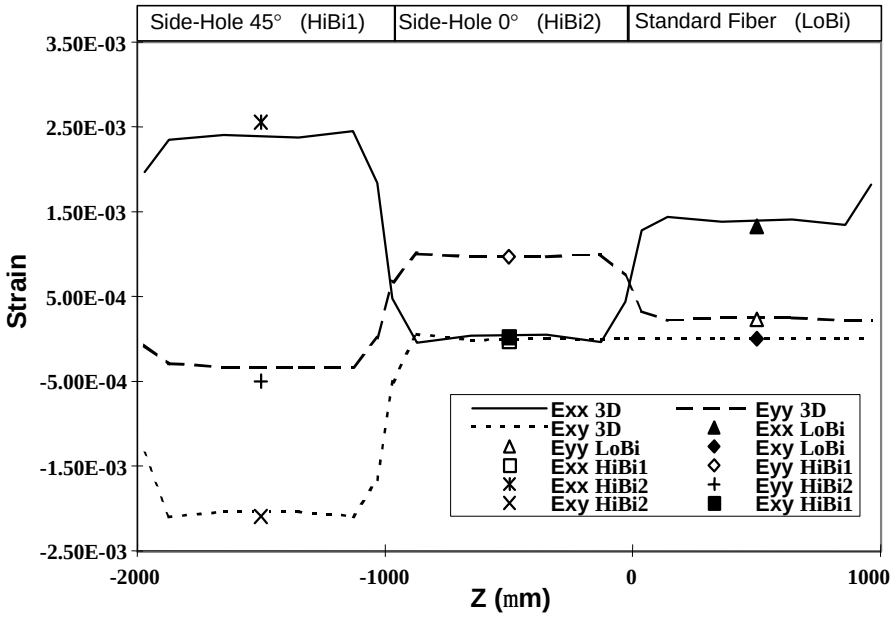

Figure 5. Strain distribution along fiber due to tension in *x*-direction.

The strains resulting from plane strain 2D models of the same fiber optic/composite system are also plotted in the same graph. A comparison of the 2D strains and the average strains produced by the 3D model shows general agreement to within 5% except for the shear strain in the 45° side-hole fiber for the in-plane shear loading, where the discrepancy is 12.8%. Analysis of uniform tension in the *y*-direction and shear in *x*-*y* plane were also investigated, and lead to the same conclusions as described above. These comparisons confirm the adequacy of using 2D analysis to examine the strain state in the multi-axis sensor.

3.2 Transformation between measured strains and strains in the far-field host material

This section uses 2D finite element analysis to find the transformations between the strains in host composite and the strains in the cores of the respective IFP segments. When the sensor is embedded into structures, the stress and strain distribution at that point is disturbed, no matter how small the sensor. A transformation between the measured strains in the fiber sensor and average strains far away from the embedded sensor are therefore required. This is done by analyzing the strains in a representative volume element (RVE) of the composite material containing the embedded sensors. This RVE is used to determine the required transformation between the far-field strains in composite and the core strains following the philosophy of Ref. [2].

The strain in fiber direction (z-direction, measured by ILFE sensor) is assumed to be the same for all the fiber segments, and also the same as the host material, leaving only the transformation matrices for the circular core and side-hole fiber to be determined. To obtain the transformation matrix, strain states both in the far-field host material and in the sensor are needed [13]. For 2D problems, two uniform tensions and a in-plane shear case are the simplest combination of stress states that lead to the desired transformations.

3.3 Transformation from phase change to strains in far-field host material

With the help of the transformation between sensor strains and strains in the far-field, we can calculate the structural strains from the measured phase change directly. The measured phase changes can be related to core strains as

$$\Delta f^{ILFE} = k_1 e_1 \tag{4}$$

$$\begin{aligned} \Delta f^{L} &= k_{21} e_1 + k_{22} e_2^{L} + k_{23} e_3^{L} \\ \Delta f^{0} &= k_{31} e_1 + k_{32} e_2^{0} + k_{33} e_3^{0} \\ \Delta f^{45} &= k_{41} e_1 + k_{42} e_2^{45} + k_{43} e_3^{45} \end{aligned} \tag{5}$$

where e_1 is the axial strain, e_2 and e_3 are the secondary principal strains in fiber cores, superscripts *L*, *0*, and *45* indicate the circular core fiber, and 0^o and 45^o oriented side-hole fibers, respectively, and k_{ij} (*i, j = 1, 2, 3*) are strain coefficients. Eqs. (4) and (5) form the basis for a system of equations which relate the measured phase changes in each of the four elements of the sensor and the far-field host strain state. Note however, that the strains in Eqs. (4) and (5) refer to the strains in the respective fiber cores, therefore the transformations between the host strains and fiber strains developed in the previous section must be used to develop a transformation between the measured phase change and the far-field strains in the composite structure.

It can be shown that the transformations are three linear equations that can be used to find the strains ε_x , ε_y , and ε_{xy} in the host material, if the phase changes $\Delta\phi^{L}$, $\Delta\phi^{0}$, and $\Delta\phi^{45}$ in the cavities are measured [13].

4 CONCLUSION

This paper has presented an orthogonal strain sensor based on optical fiber technology. The optical arrangement of the three-strain sensor system, including the technical approach, and fabrication of the micro-cavity sensors have been discussed in detail. The finite element method has been applied to the multi-strain sensor to develop a relationship between the strains in the fiber sensor and the far-field strains in the host material. The 2D finite element analysis model results showed that with different loading cases the strains in the side-hole PANDA-like fiber indicated significant core strain and was used to design the placement and diameters of the side holes to maximize transverse strain sensitivity. The results of comparing 2D and 3D FEM models show that the replacing of 3D

model with 2D models gives accurate in-plane strains. The transformations between the phase changes $\Delta\phi^L$, $\Delta\phi^0$, and $\Delta\phi^{45}$ in the cavities and the strains ε_x , ε_y , and ε_{xy} in the host material can be expressed by three linear equations.

ACKNOWLEDGEMENTS

This work has been made possible with the financial support of Wright Laboratory (Contract No. F33615-95-C-3401 and technical monitor of Mr. Greg Czarnecki. The contribution of Naval Research Lab to help us draw side-hole fibers is particularly acknowledged.

REFERENCE

[1] J.S. Sirkis and Y.L. Lo, “Simultaneous Measurement of Two Strain Components Using 3x3 and 2x2 Coupler-Based Passive Demodulation of Optic Fiber Sensors,” *Journal of Lightwave Technology*, Vol. 12, No. 12, pp. 2153-2161, 1997.

[2] X.D. Jin, J.S. Sirkis, and J.K. Chung, “Simultaneous Measurement of Two Strain Components in Composite Structures Using Embedded Fiber Sensors,” *Journal of Composite Material*, Vol. 33, No. 15, pp. 1376-1387, 1999.

[3] E. Udd, C.M. Laurence, and D.V. Nelson, “Development of a Three-Axis Strain and Temperature Fiber Optic Grating Sensor,” *Proc. SPIE*, Vol. 3042, pp. 229-236, 1997.

[4] T. Rossmanith, X.D. Jin, J.S. Sirkis, M.K. Park, V. Venkat, and B.D. Prasad, “Manufacturing of Core Mirrors for Intrinsic Fabry-Perot Interferometers Using Sol-Gel Process,” *Proc. SPIE* Vol. 3670, pp. 34-40, 1999.

[5] J.S. Sirkis, M.A. Putman, T.A. Berkoff, D.D. Brennan, and E.J. Friebele, “In-Line Fiber Etalon for Strain Measurement,” *Proc. SPIE*, Vol. 2191, pp. 137-147, 1994.

[6] H.M. Xie, Ph. Dabkiewicz, and R. Ulrich, “Side Hole Fiber for Fiber-Optic Pressure Sensing,” *Optics Letters*, Vol. 11, No. 5, pp. 333-335, 1986.

[7] S. Tanaka, K. Yoshida, S. Kinugasa, and Ohtsuka, “Birefringent Side-Hole Fiber for Use in Strain Sensor, ” *Optical Review*, Vol. 4, No. 1A, pp. 92-95, 1997.

[8] F. Farahi, T.P. Newson, J.D. Jones, and D.A. Jackson, " Coherence Multiplexing Of Remote Fiber Optic Fabry-Perot Sensing Systems," *Optics Communications*, Vol. 65, No. 5, pp. 319-321, March 1988.

[9] Y.L. Lo, and J.S. Sirkis, "Passive demodulation techniques for Michelson and polarimetric optical fiber sensors," *Experimental Techniques*, Vol.19, no.3, pp. 23-27, 1995.

[10] A. Friedberger and R.S. Muller, “Improved Surface-Micromachined Hinges for Fold-Out Structures, ” *Journal of Microelectromechanical systems*, Vol. 7, No. 3, September 1998.

[11] M.J. Daneman, N.C. Tien, O. Solgaard, A. Pisano, K.Y. Lau, and R.S. Muller, “Linear Microvibromotor for Positioning Optical Components, ” *Journal of Microcelectromechanical systems*, Vol. 5, No. 3, September 1996.

[12] J.S. Sirkis, and H.W. Haslach, “Complete Phase-Strain Model for Structurally Embedded Interferometric Optical Fiber Sensors,” *Journal of Intelligent and Material System and Structure*, Vol. 2, No. 1, pp. 3-24, 1991.

[13] X.D. Jin, T. Rossmanith, J.S. Sirkis, A. Dasgupta, D. DeVoe, F.F. Rosenberger III, V.S. Venkat, Y.C. Shi, and C. Askins, " Progress Towards an Orthogonal Strain State Sensor Based Optical Fiber Technology," *SPIE Vol.* 3670, pp. 516-531, 1999.

AUTHORS: T. ROSSMANITH, X.D. JIN and J.S. SIRKIS, Smart Materials and Structures Research Center, University of Maryland at College Park, College Park, MD 20742, USA